

Preparation and Voltammetric Studies of Titanium (IV) Phosphate Modified with Silver Hexacyanoferrate to a Voltammetric Determination of L-Cysteine

Loanda Raquel Cumba, Urquiza de Oliveira Bicalho, Devaney Ribeiro do Carmo*

Faculdade de Engenharia de Ilha Solteira UNESP - Univ Estadual Paulista, Departamento de Física e Química, Av. Brasil Centro, 56 CEP 15385-000, Ilha Solteira, SP, Brazil. fax: +55 (18)3742-4868

*E-mail: docarmo@dfq.feis.unesp.br

Received: 9 March 2012 / Accepted: 4 April 2012 / Published: 1 May 2012

In this work, a novel Titanium (IV) Phosphate (TiPh) composite was prepared using a easily methodology of the synthesis. A preliminary characterization of the precursor and resulting materials was defined using spectroscopic and voltammetric techniques. As a second step, TiPh was reacted with silver ions (TiPhAg) and subsequent hexacyanoferrate was added (TiPhAgHCF). The electrochemical behaviour of the composite (TiPhAgHCF) was verified by means of a graphite paste electrode using cyclic voltammetry in a potential range of 0.2 to 0.9 V (*vs* Ag/AgCl). The cyclic voltammogram of the modified electrode containing (TiPhAgHCF) exhibited a single redox couple. The redox couple present a formal potential (E^{θ}) of 0.77 V *vs* Ag/AgCl (KNO₃ 1.0 mol L⁻¹; $\nu = 20$ mV s⁻¹) and ascribed to the [Fe^{II}(CN)₆] / [Fe^{III}(CN)₆] processes. In a electroanalytical study, the peak located at 0.77 V present a sensitive response to L-cysteine. The modified graphite paste electrode showed a linear range from 2.0×10^{-4} to 9.0×10^{-3} mol L⁻¹ for the determination of L-cysteine with a limit detection of 3.34×10^{-4} mol L⁻¹ and relative standard deviation of $\pm 5\%$ ($n = 3$) and amperometric sensitivity 10.34×10^{-3} A mol L⁻¹. The modified electrode was electrochemically stable and showed excellent reproducibility.

Keywords: Titanium (IV) phosphate, cyclic voltammetry, L-cysteine

1. INTRODUCTION

Crystalline titanium phosphate is a widely amphoteric inorganic material which shows good biocompatibility, stability and environmental safety. The surface property of Crystalline Titanium phosphates is particularly important in determining the bio and photocatalytic reaction kinetics, mechanisms because these reactions mostly take place on the surface [1]. Each surface modification

method has its unique role in affecting the kinetics and mechanisms of catalytic reactions. Therefore, combining two different modification methods on the same catalyst particle may obtain synergic effects with taking advantage of each method and a new chemical property can lead.

The majority studies centered around the different aspect usually involving bio and photocatalytic activity fields [2-7] and a promising aspect is its use as an inorganic ion exchanger and sorbent [8-9] due to its high chemical stability and high ion exchange capacity, which may find application in solid phase extraction (SPE). It was suggested that the sorption properties of titanium phosphate sorbents can be improved by modifying them with transition metal cations, which are amphoteric and differ from titanium (IV) in electronegativity [10]. An excellent review about investigations devoted to the synthesis of nanopowders and films of titanium oxide for photocatalysis was recently published [11]. In the electrochemical field, the preparation of Titanium chemically modified electrode surface is a subject under active study in recent years. Numerous ways for anchoring electrochemically active compounds onto electrode surfaces have been investigated aiming the shortening of the distance between the redox sites involved in the electron transfer reaction [12].

In this work we report the voltammetric studies resulting from the direct preparation of Titanium (IV) Phosphate (TiPh) from aqueous phosphoric acid and Titanium (IV) isopropoxide. This method is characterized by its simplicity in composite preparation. The material obtained from Titanium (IV) Phosphate (TiPh) was treated with AgNO_3 (TiPhAg) then the solid supported was submitted to a reaction with hexacyanoferrate to give rise to a new hybrid material (TiPhAgHCF, where AgHCF means silver hexacyanoferrate), which is a Prussian Blue analog, widely used for several electrocatalytical applications [13]. The idea is to combine the ion exchange properties with good ionic conductor of TiPh and this combination will facilitate charge transfer between AgHCF and TiPh due to the cation diffusion within the AgHCF mediated by TiPh component. In this paper the novel material, after initial optimization conditions, was tested in the electrocatalysis of L-cysteine.

L-Cysteine (1-2-amino-3-mercaptopropionic acid) is a sulfur-containing molecule. The sulphhydryl (-SH) group of cysteine plays a key role in the biological activity of protein and enzymes. It is widely present in many medicines, food and biological tissues, such as cysteine protease, vasopressin and anti-diuretic hormone and is one of the most important amino acids [14,15]. In the last years, Metal hexacyanoferrate (MHCF) [16-26] and its analogue Metal Nitroprusside [27-30] modified electrodes have been investigated intensively for a variety of application areas including electrocatalysis for determination of L-cysteine. The vast majority of these MHCF modified electrodes employed for the determination of cysteine is based on amperometric method however, to the best of our knowledge, there is no report for a direct voltammetric determination of L-cysteine employing Titanium Phosphate modified with silver hexacyanoferrate (TiPhAgHCF).

2. EXPERIMENTAL

2.1. Reagents

All reagents were analytical grade (p.a Merck) and deionized water, with Milli-Q Gradient system from Millipore was used. The solutions of L-cysteine were prepared immediately before use.

2.2. Techniques

2.2.1. Fourier transform infrared spectra

Fourier transform infrared spectra were recorded on a Nicolet 5DXB FTIR 300 spectrometer. Approximately 600 mg of KBr was grounded in a mortar with a pestle, and sufficient solid sample was grounded with KBr to make a 1wt % mixture to produce KBr pellets. After the sample was loaded, the sample chamber was purged with nitrogen for at least 10 min. prior the data collection. A minimum of 32 scans was collected for each sample at a resolution of 4 cm^{-1} .

2.2.2. X ray diffraction

The X ray diffraction patterns (XRD) were obtained using a Siemens D 5000 diffractometer with $\text{CuK}\alpha$ (λ 1.5406 Å radiation), submitted to 40 kV, 30 mA, 0.05° s^{-1} and exposed to radiation from 5 up to 80° (2θ).

2.2.3. Surface area and Porosity

The surface area and Porosity were determined at 77 K using a Micromeritics ASAP 2010 instrument. The surface area was calculated using the BET (Brunauer, Emmett, and Teller). The pore diameter distributions were calculated with the BJH (Barrett, Joyer and Halenda) method.

2.2.4. Electrochemical measurements

For cyclic voltammetric measurements was employed a potentiostat from Microchemistry, MQP1 model. The electrochemical system used was composed of three electrodes: platinum electrode used as auxiliar, $\text{Ag}/\text{AgCl}_{(s)}$ as a reference and modified graphite paste as a working electrode. The working electrode consists of a glass tube with 15 cm long, with a inner diameter of 0.30 cm and external diameter of 0.5 cm with the internal cavity connected by a copper wire to establish the electrical contact.

The cyclic voltammetry technique was employed to study the electrochemical behavior of titanium (IV) phosphate modified with silver hexacyanoferrate. The catalytic current was established by the difference between the current measured in the presence of L-cysteine and in its absence. The solutions were bubbled with nitrogen for 10 minutes before the measurements.

2.2.5. Preparation of graphite paste electrode modified with TiPhAgHCF

The graphite paste modified with TiPhAgHCF was prepared from a mixture containing of 20 mg TiPhAgHCF with 80 mg graphite powder (Aldrich) and 30 μL of mineral oil.

2.2.6. Preparation of titanium (IV) modified with phosphoric acid (TiPh)

The synthesis of titanium phosphate [17] was performed as described below: in a round-bottom flask was added 35ml of phosphoric acid P.A. (85%), 20 mL of titanium isopropoxide (IV) and 10 mL deionized water under strong agitation. The turbid solution formed was allowed to stand in the dark for one day. After the solid phase formed, it was separated by a sintered plate funnel and dried at room temperature. The material was stored in desiccators and described as TiPh.

2.2.7. Complex formation with the TiPh

The preparation of the binuclear complex has been prepared in two steps; initially it was added 2.0 g of TiPh into 50mL of 1.0×10^{-2} mol L⁻¹ of silver nitrate (50% ethanol / water). This mixture was stirred for 60 minutes at room temperature and solid phase was then filtered and washed thoroughly with ethanol / water mixture several times, the prepared material was dried at temperature above 70 °C. The material was described as TiPhAg. In a second step, the TiPhAg was added to an aqueous solution containing 1.0×10^{-3} mol L⁻¹ potassium ferricyanide (K₃[Fe(CN)₆]). The solution was stirred for 2 hours then the precipitate was filtered, washed exhaustively with deionized water and dried at room temperature. The material formed was described as TiPhAgHCF.

3. RESULTS AND DISCUSSION

The silver ion forms insoluble polymeric complexes with iron (II) and iron (III) hexacyanides [31,32]. These complex compounds presents a stoichiometry and structure analogous to the iron blues (i.e., Prussian blue), consisting of a basic face centered-cubic polymeric network (possibly disordered) with the remaining charge-balancing ions, and water, occupying undetermined lattice sites [33]. Like Prussian blue, the crystalline structure of TiPhAgHCF also admit potassium ion to charge-balancing

The X-rays diffractogram of TiPh illustrated by Figure 1(a) was analyzed by Search-Match software in order to elucidate the crystalline characteristic of the compound formed in the new synthetic route proposed. The four intense peaks found in the diffractogram are located at 11.59; 20.70; 25.62 and 35.69 degrees. Through of XRD patterns analyzed by the software, was concluded that these peaks are characteristic of the Ti₃(PO₄)₄ compound which form the database of Search-Match is JCPDS # 52-327. Figure 1 (b) shows a diffractogram of TiPhAgHCF containing seven peaks 12.27; 19.20; 24.62; 28.44; 29.51; 32.11 and 38.75. In both materials two peaks near at 2θ 25.0 and 2θ 27.0° which correspond to anatase and rutile phases were observed [34]. Figure 2 (c) show the spectrum in the infrared region of TiPh, it was detected a broad band in the region of 3400 cm⁻¹ which was attributed to symmetrical and asymmetrical –OH stretch, there is also a narrow and medium band in 1620 cm⁻¹ that was assigned to H–O–H bond of water and a strong absorption at 1035 cm⁻¹ which was attributed to ν (P=O) stretching. The band observed at 1400 cm⁻¹ was attributed to δ (POH) stretching [4,35]. The bands presented with values of 518 and 607 cm⁻¹ correspond to links O–Ti–O [36].

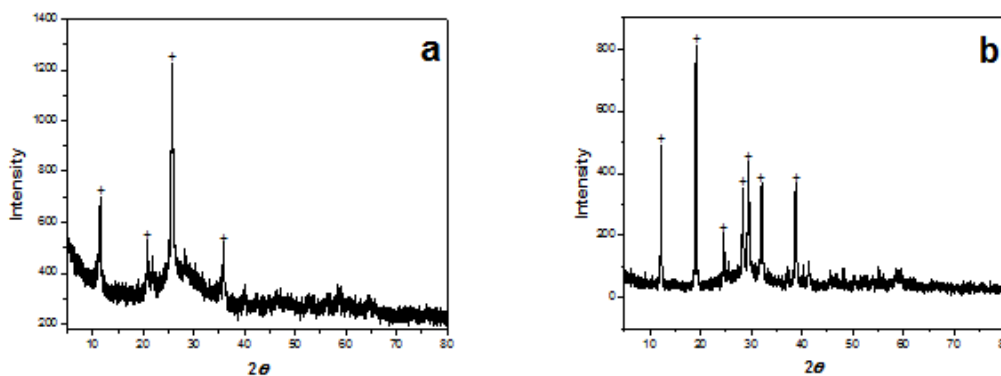


Figure 1 X-ray diffractogram of: (a)TiPh and (b) TiPhAgHCF

Figure 2 (c) illustrates the infrared spectrum of TiPh after silver adsorption (TiPhAg) and the reaction between TiPhAg and potassium hexacyanoferrate(III) (TiPhAgHCF) was showed in Figure 2 (b). The spectra (c) and (b) showed the same peaks observed in spectrum (c) except for a peak at 2120 cm^{-1} found only on the curve (b). This peak, assigned to $\nu(\text{C}\equiv\text{N})$ stretching confirms the formation of silver hexacyanoferrate composite [37] formed after reaction of the starting material TiPh. This peak is 86 cm^{-1} shifted with to higher energy with relation to potassium hexacyanoferrate (Fig. 2(a)).This behavior is in according to one described in the literature [37] and is attributed to both the kinematic coupling that occurs when a second mass is attached to the CN unit as well as to the fact that the N lone pair is antibonding with respect to the $\text{C}\equiv\text{N}$ bond [38].

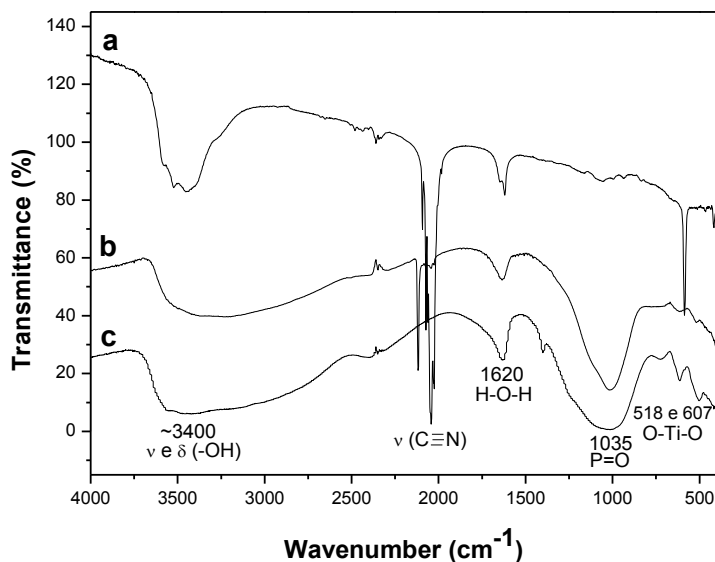


Figure 2. Infrared spectrum of: (a) HCF, (b) TiPhAgHCF and (c) TiPh

Figure 3(b) shows the adsorption-desorption isotherm for TiPh according to the method proposed by Brunauer, Emmett, and Teller (BET). This hysteresis type IV–H3, which is associated

with non-uniform multilayer adsorption on the porous surface, but very different from the hysteresis type III–H1 observed for the commercial TiO₂ (Figure 3(a)), characteristic of compounds agglomerate or compacts, of semi uniform spheres and narrow distribution of pore size [39].

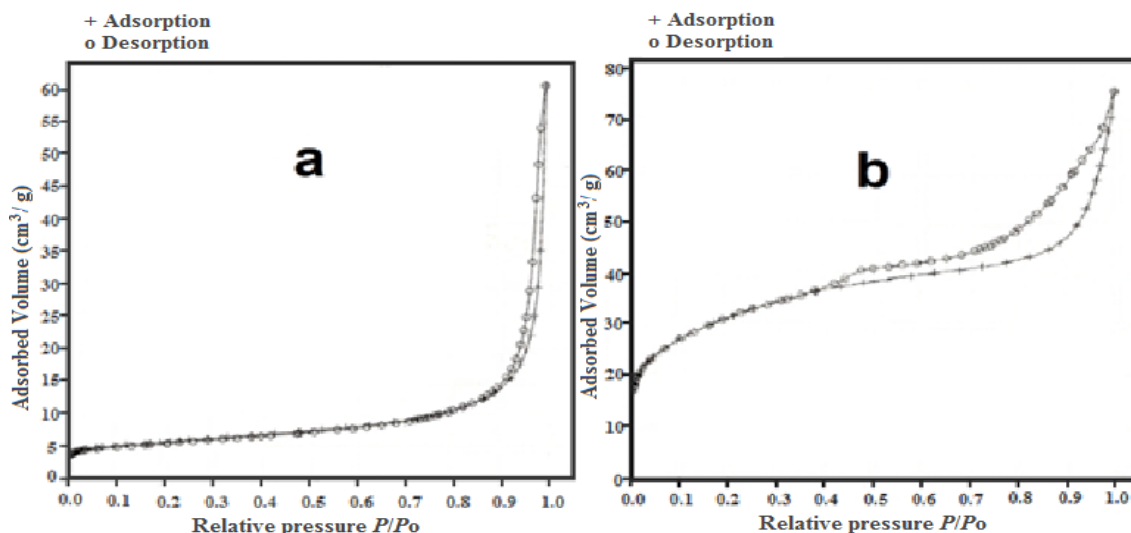


Figure 3. Nitrogen sorption isotherms of: a) TiO₂ e b) TiPh

Table 1 lists the main parameters of these studies. According to Table 1, there was an increase in surface area of TiO₂ compound to the TiPh around 100 m² g⁻¹ this increase makes the application of this material in adsorption studies becomes very interesting. According to the large surface area obtained, many active sites can be found for adsorption of the cations under investigation. High surface areas also are interesting for application in chemically modified electrodes. It is also noticed an increase in pore volume and a decrease in average pore size.

Table 1. Structural parameters of TiO₂ and TiPh.

Sample	Surface area (m ² g ⁻¹)	Pore volume (cm ³ g ⁻¹)	Average size of the pore 4V/A
TiO ₂	6.4164	0.0020	235.8848
TiPh	95.8649	0.0500	46.8081

3.1. Electrochemical characterization of TiPhAgHCF

Through the cyclic voltammogram of the modified electrode with graphite paste (20% m/m), it can be observed only a well-defined redox couple with an average potential $(E^{\theta})_1 = 0.77$ V vs Ag/AgCl (KNO₃ 1.0 mol L⁻¹; $v = 20$ mV s⁻¹) which was attributed to the redox process [Fe^{II}(CN)₆] / [Fe^{III}(CN)₆] of the binuclear complex formed. This formal potential is in concordance with the value previously reported for silver hexacyanoferrate modified electrodes [40]. One major difference of the

others metal hexacyanoferrates is the pronounced asymmetry of the oxidation as compared to the reductive wave. It will be shown that the lower peak current and broad tail for the oxidation of silver ferrocyanide are essentially kinetic effects [37].

3.2. Study on the effect of cations and anions

The oxidation and reduction process of the modified compounds on the TiPhAgHCF surface occurs initially by the equilibrium between the electrolyte solution cation and the electrode surface [36,41]. The nature of the electrolyte solution cation employed showed great influence on the current intensity and ($E^{0'}$). With the use of the base electrolyte alkali metal chloride, a drastic decrease in current density and a total disappearance of the peak were observed. This effect was attributed to the formation of AgCl which blocks the electron transfer process on the electrode surface as illustrated in Figure 4. This behavior was also reported by Jay [42].

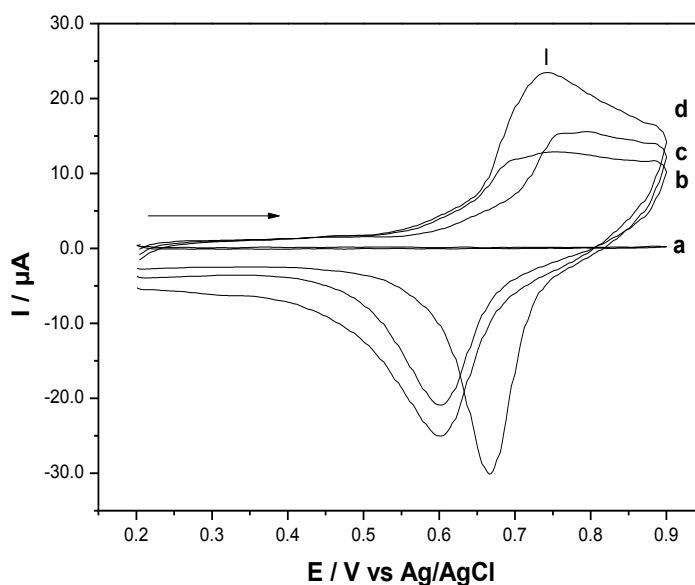


Figure 4. Cyclic voltammogram of graphite paste modified with TiPhAgHCF in different electrolytes (a) KCl, (b) NaNO₃, (c) KNO₃ and NH₄NO₃ ($\nu = 20 \text{ mV s}^{-1}$)

Studies performed with different cations of the nitrate showed that not only the current intensity as well as the average potential of redox couple processes ($E^{0'}$) are influenced by the cation nature, and these potentials are shifted to more anodic regions in the following sequence: $\text{K}^+ > \text{Na}^+ > \text{Li}^+$. The cation effect on the cyclic voltammograms of TiPhAgHCF are illustrated by Figure 5.

Table 2 lists the main electrochemical parameters of the compounds mentioned above and their radii of hydration. Compounds such as Prussian Blue and similar structures that exhibit zeolitic cavity, in other words, channels that allow the insertion of small molecules and ions behaves as zeolites [41,42]. Because they have smaller radii of hydration, K^+ and NH_4^+ is more easily lodge in the pores of the zeolite structure. Due to a higher affinity of these cations, was observed, as shown in the

voltammograms of Figure 5, a better electrochemical response of electrode graphite paste modified with TiPhAgHCF in the presence of electrolyte containing cations K^+ and NH_4^+ , the cation K^+ has a better voltammetric performance in relation to the cation NH_4^+ , although almost the same hydrated radius, this can be explained by the cation NH_4^+ present a low ion mobility in relation to K^+ [41].

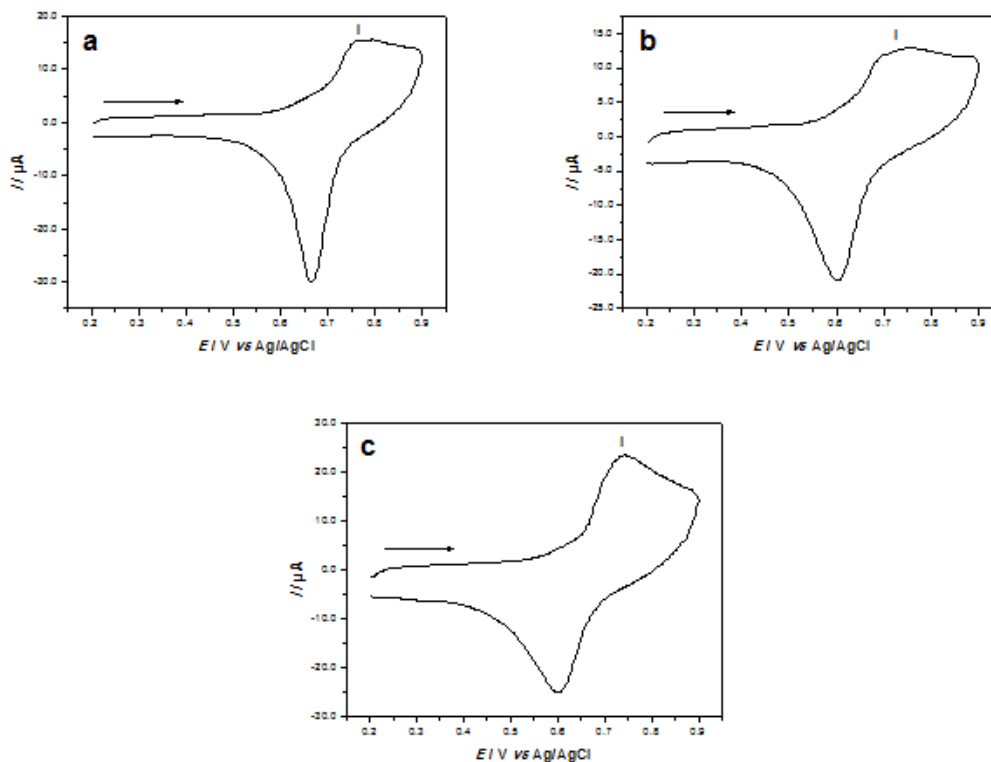


Figure 5. Cyclic voltammogram of graphite paste modified with TiPhAgHCF in different electrolytes (a) KCl, (b) NaNO₃, (c) KNO₃ and NH₄NO₃ ($v = 20 \text{ mV s}^{-1}$)

Table 2. Main voltammetric parameters of TiPhAgHCF in the presence of different supporting electrolytes.

Cation	(I _{pa} /I _{pc}) ₁	*(E ⁰) ₁ (V)	*(ΔE _p) ₁ (V)	Diameter of the cation hydrated (nm)
NH ₄ ⁺	0.66	0.67	0.14	0.245
Na ⁺	0.26	0.68	0.15	0.360
K ⁺	0.25	0.77	0.10	0.240

$$E^{0'} (V) = (E_{pa} + E_{pc})/2 \text{ e } \Delta E_p (V) = |E_{pa} - E_{pc}|$$

Figure 6 illustrates the cyclic voltammograms at different concentrations of KNO₃ (1.0×10^{-3} to 1.0 mol L^{-1}), peak I showed a shift potential ($E^{0'}$) to more positive values with increasing concentration

of electrolytes. Increasing the concentration of KNO_3 observed the participation of the K^+ ion in the redox process, where the shift of potential is attributed to the change in the activity of these ions [41].

For the graphite paste electrode modified with TiPhAgHCF the slope of this line was 25 mV per decade concentration of potassium ions concentration indicating an almost Nernstian process [41] and two electrons are involved. Similarly to the modified electrode with TiPhCuHCF response where an almost nernstian behavior was an indication of participation of potassium ions in the redox process. The dependence of the potential ($E^{0'}$) with the electrolyte concentration can be explained by the charge balance between the cation and TiPhAgHCF, similar results had been described in a previous publication to an analogue compound TiPhCuHCF [17].

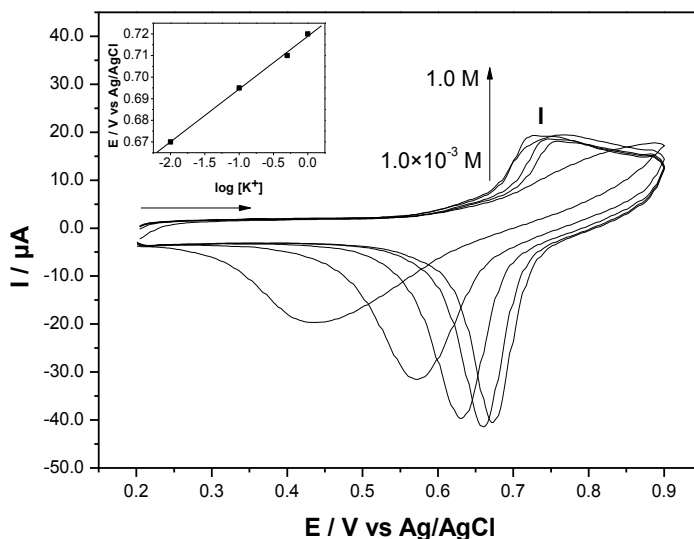


Figure 6. Cyclic voltammogram of carbon paste electrode modified with TiPhAgHCF in several concentrations ($1.0 \times 10^{-3} - 1.0 \text{ mol L}^{-1}$). (Inserted graphic: Average potential ($E^{0'}$) of graphite paste modified with TiPhAgHCF a function of log concentration of KNO_3)

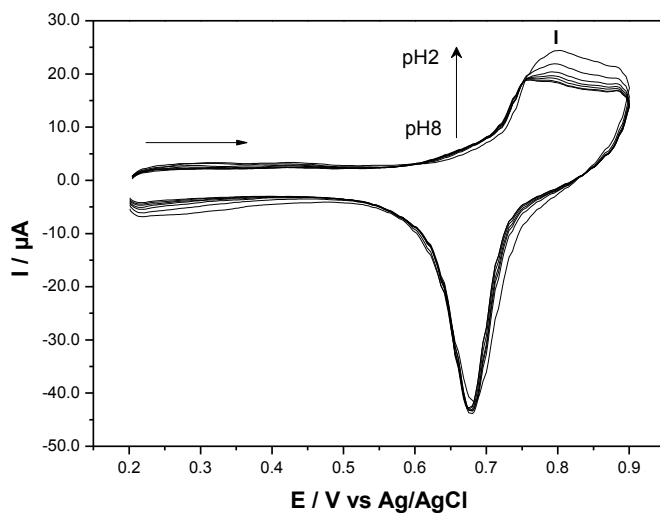


Figure 7. Cyclic voltammogram of graphite paste modified with TiPhAgHCF to different pH values (2 - 8); ($\text{KNO}_3 1.0 \text{ mol L}^{-1}$, $\nu = 20 \text{ mV s}^{-1}$)

Figure 7 shows the cyclic voltammogram at different pH values (2 - 8). With the increase in hydrogen ion concentration, there was a small increase in the current intensity for the redox process. Therefore, from pH < 4, the redox process, became more distinct, which can be explained by the presence of high concentrations of H⁺ ions, which governs the electroactivity of one or more forms of intermediate species due a probable intercalation of H⁺ ions into de metal hexacyanoferrates and the anodic potential shift to more positive potentials [17].

Figure 8 illustrates the cyclic voltammogram of TiPhAgHCF, respectively, at different scan rate (20 - 100 mV s⁻¹). With increasing scan rate, we observed a linear dependence between the intensity of the anodic peak current and scan rate for peak I, typical of surface confined species [43].

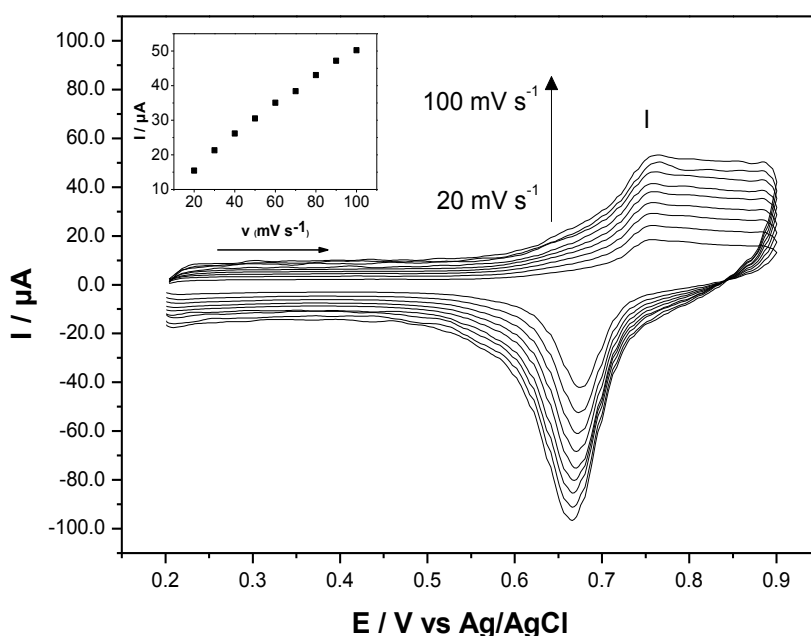


Figure 8. Cyclic voltammogram of TiPhAgHCF different scan rates: 20 - 100 mV s⁻¹; (KNO₃ 1.0 mol L⁻¹; pH 7.0). (Inserted graphic: Dependence of current peak I (anode and cathode) with the square root of scan rate

Based on the results above, was chosen KNO₃ (1.0 mol L⁻¹, pH 7.0; $v = 20 \text{ mV s}^{-1}$) to be used in subsequent voltammetric investigation.

Figure 9 illustrates the performance of the graphite paste electrode with TiPhAgHCF in KNO₃ solution 1.0 mol L⁻¹. The voltammogram in the absence (curve a) and presence (curve b) of $9.0 \times 10^{-3} \text{ mol L}^{-1}$ L-cysteine assigned to bare graphite paste electrode showed no electroactivity in the potential range studied (0.2 to 0.9 V). The graphite paste electrode modified with TiPhAgHCF in the absence of L-cysteine was showed in curve c. In addition, it was observed that in the presence of $9.0 \times 10^{-3} \text{ mol L}^{-1}$ of L-cysteine the current of peak increases as illustrates the curve d.

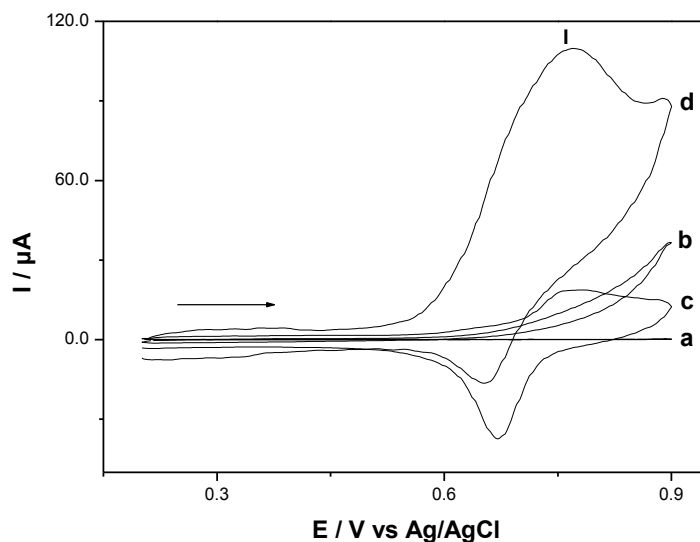


Figure 9. Cyclic voltammogram of: a) graphite paste electrode; b) graphite paste electrode in 9.0×10^{-3} mol L⁻¹ L-cysteine; c) graphite paste electrode modified with TiPhAgHCF; d) graphite paste electrode modified with TiPhAgHCF and 9.0×10^{-3} mol L⁻¹ L-cysteine (KNO₃ 1.0 mol L⁻¹ ; $\nu = 20$ mV s⁻¹)

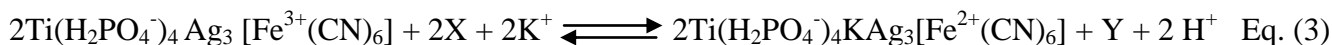
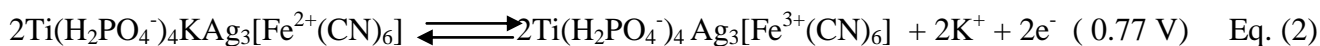
The intensity of the anodic peak current increases proportionally with the concentration of L-cysteine as shown in Figure 10. This increase occurs due the electrocatalytic oxidation of L-cysteine by the electron mediator TiPhAgHCF.

The Equation for the electrochemical oxidation of L-cysteine as described in the literature [44] can be represented as follows:



Therefore, in view of this reaction of L-cysteine, the oxidation of L-cysteine on the surface of the graphite paste electrode modified with TiPhCuHCF can be represented according to the equations 1, 2 and 3:

The oxidation of L-cysteine on the surface of the graphite paste electrode modified with TiPhAgHCF can be represented according to Equations 2 and 3 by analogy one recently described [17]



where X = L-cysteine ; Y = L-cystine

Figure 10 illustrates the voltammogram when the concentration of L-cysteine is changed. It was observed through these studies that the current for peak I ($(E^{0'})_1 = 0.77$ V) increases in accordance with the increase of concentration of the drug. Thus, it was determined that with the addition of aliquots of the L-cysteine, the drug was oxidized by an electrocatalyst oxidation process on the electrode surface. The electrocatalytic oxidation of L-cysteine occurs as follows: Fe^{3+} produced during anodic scan, chemically oxidize the molecule L-cysteine when it is reduced to Fe^{2+} , which will again be electrochemically oxidized to Fe^{3+} .

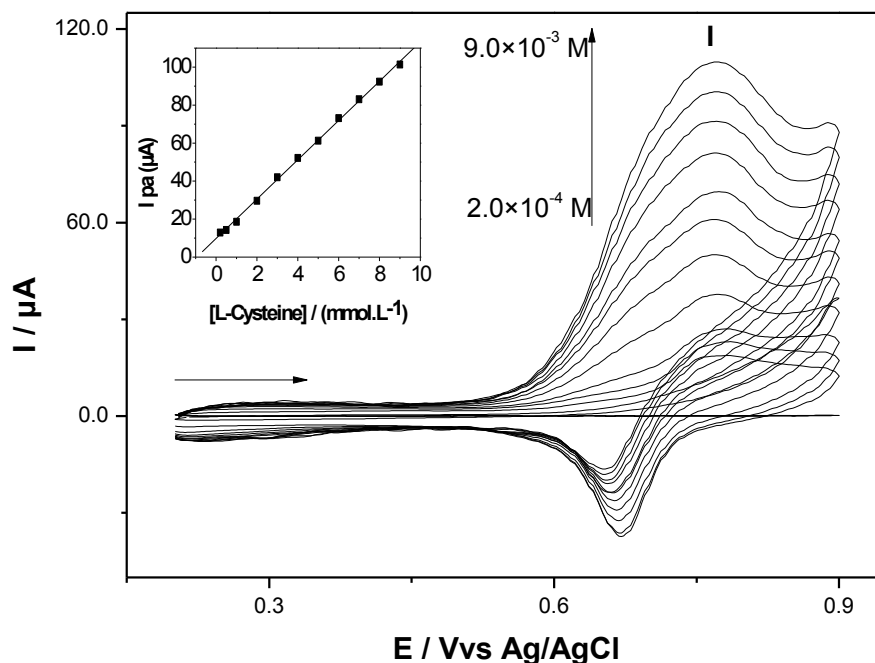


Figure 10. Cyclic voltammograms of the applications of various concentrations of L-cysteine using a carbon paste electrode modified with TiPhAgHCF (KNO_3 1.0 mol L^{-1} ; $\nu = 20$ mV s^{-1}). (Inserted graphic: Analytical curve of the anodic peak for the determination of L-cysteine using a carbon paste electrode modified with TiPhAgHCF (KNO_3 1.0 mol L^{-1} , pH 7.0; $\nu = 20$ mV s^{-1})

Thus L-cysteine is oxidized at the electrode surface, and this process occurs in the potential of 0.77 V. The oxidation process does not occur in this potential when is used glassy carbon electrode or unmodified carbon paste. The peak potential is not affected by the concentration of L-cysteine and the catalytic current is also linear with the square root of scan rate. The behavior of electrochemical oxidation of L-cysteine in the TiPhAgHCF modified electrode is very similar to the electrode modified with a film of Prussian blue, which shows an increase of the current in the two oxidation potentials (0.79 V) in the presence of L-cysteine (1.0 mol L^{-1} KCl, pH 7.0 vs. Ag / AgCl) [43].

Figure 10 (inserted graphic) illustrates the analytical curve used to determine L-cysteine. The modified electrode showed a linear response from 2.0×10^{-4} to 9.0×10^{-3} mol L^{-1} with the corresponding equation $Y(\mu\text{A}) = 9.82 + 10.344 \times 10^3 [\text{L-cysteine}]$, and a correlation coefficient of $r = 0.9992$. The method showed a detection limit of 3.34×10^{-4} mol L^{-1} with a relative standard deviation of $\pm 5\%$ ($n = 3$) and amperometric sensitivity of 10.34×10^{-3} A mol L^{-1} .

4. CONCLUSION

Titanium (IV) Phosphate (TiPh) was prepared using a new methodology of the synthesis. The cyclic voltammogram of the modified electrode containing (TiPhAgHCF) exhibits one redox couple. The redox couple present a formal potential ($E^{0'}$) of 0.77 V ascribed to $\text{Fe}^{\text{II}}(\text{CN})_6 / \text{Fe}^{\text{III}}(\text{CN})_6$ processes. The redox process presented by the graphite paste electrode modified with TiPhAgHCF shows electrocatalytic activity for the oxidation of L-cysteine. The linear range for the determination of L-cysteine was found to be $2.0 \times 10^{-4} - 9.0 \times 10^{-3} \text{ mol L}^{-1}$ showing a detection limit of $3.34 \times 10^{-4} \text{ mol L}^{-1}$ and amperometric sensitivity $10.34 \times 10^{-3} \text{ A mol L}^{-1}$.

The determination of L-cysteine is a direct application of graphite paste electrode modified with TiPhAgHCF. When compared to other electroanalytical methods, the main advantage of the modified electrode TiPhAgHCF is the facility of manufacture and the fact that its surface can be easily renewed. This feature is important when one wants to effectively implement various measurements in a short period of time. Another advantage is that it needs no prior chemical treatment.

ACKNOWLEDGEMENT

Financial support for this research was supplied by Fundação de Amparo à Pesquisa do Estado de São Paulo (FAPESP- Proc.03/12882-6) and Coordenação de Aperfeiçoamento de Pessoal de Nível Superior (CAPES).

References

1. B.D. Yao, Y.F. Chan, X.Y. Zhang, W.F. Zhang, Z.Y. Yang and N. Wang, *Appl. Phys. Lett.* 82 (2003) 281
2. G.F. Fu, P.S. Vary and C.T. Lin, *J. Phys. Chem. B* 19 (2005) 8889
3. Z.Y.U. Yuan and B.L. Su, *Colloids Surf. A* 241 (2004) 173
4. W. Zhang, L. Zou and L. Wang, *Appl. Catal. A* 371 (2009) 1
5. A.Zielinska, E. Kowalska, J.W. Sobczak, I. Łacka, M. Gazda, B. Ohtani, J. Hupka and A.Zaleska, *Sep. Purif. Technol.* 72 (2010) 309
6. R.A. Lucky and P.A. Charpentier, *Appl. Catal. B* 96 (2010) 516
7. U.G. Akpan and B.H. Hameed, *Appl. Catal. A* 375 (2010) 1
8. T.Y. Ma, X.J. Zhang and Z.Y. Yuan, *Microporous Mesoporous Mater.* 123 (2009) 234
9. T.Y. Ma, X.J. Zhang, G.S. Shao, J.L. Cao and Z.Y. Yuan, *J. Phys. Chem. C* 112 (2008) 3090
10. V.I. Shapovalov, *Glass Phys. Chem.* 36 (2010) 121
11. W. Song, W. Xiaohong, Q. Wei and J. Zhaohua, *Electrochim. Acta* 53 (2007) 1883
12. J.P. Launay, *Chem. Soc. Rev.*, 30 (2001) 386
13. A.A. Karyakin, *Electroanalysis* 13 (2001) 813
14. D.L. Nelson and M.M. Cox, *Lehninger Principles of Biochemistry*, 3 ed. (Worth Publishers, USA, 2000)
15. E.J. Taylor, *Dorland's Illustrated Medical Dictionary*, (WB Saunders, Philadelphia, 1988)
16. I.L. Mattos and L. Gorton, *Quim. Nova* 24 (2001) 200
17. A.R.F. Pipi and D.R. Carmo, *J. Appl. Electrochem.* 41 (2011) 787
18. L. Qu, S. Yang, G. Li, R. Yan, J. Li and L. Yu, *Electrochim. Acta* 56 (2011) 2934
19. X. Li, Z. Chen, Y. Zhong, F. Yang, J. Pan and Y. Liang, *Anal. Chim. Acta* 710 (2012) 118
20. M.R. Majidi, K. Asadpour-Zeynali and B. Hafezi, *Microchim. Acta* 169 (2010) 283

21. N. Sattarahmady and H. Heli, *Anal. Biochem.* 409 (2011) 74
22. A.A. Ensafi, S. Dadkhan-Tehrani and H. Karimi-maleh, *Anal. Sci.* 27 (2011) 409
23. A. Abbaspour and A. Ghaffarinejad, *Electrochim. Acta* 53 (2008) 6643
24. L.G. Shaidarova, S.A. Ziganshina, A.V. Gedmina, I.A. Chelnokova and G.K. Budnikov, *J. Anal. Chem.* 66 (2011) 633
25. X. Tang, Y. Liu, H. Hou and T. You, *Talanta* 80 (2010) 2182
26. H. Razmi and E. Habibi, *Electroanal.* 21 (2009) 867
27. W.T. Suarez, L.H. Marcolino and O. Fatibello-Filho, *Microchem. J.* 82 (2006) 163
28. E. Hollauer and J.A. Olabe, *J. Braz. Chem. Soc.*, 8 (1997) 495
29. D.R. Carmo, R.M. Silva and N.R. Stradiotto, *J. Braz. Chem. Soc.* 14 (2003) 616
30. D.R. Carmo, L.L. Paim, D.R. Silvestrini, A.C. Sá, U.O. Bicalho and N.R. Stradiotto, *Int. J. Electrochem. Sci.* 6 (2011) 1175
31. A. Bellomo, *Talanta* 17 (1970) 1109
32. A. Bellomo, D. DeMarco and A. Casale, *Talanta* 19 (1972) 1236
33. R.E. Wilde, S.N. Ghosh and B.J. Marshall, *Inorg. Chem.* 9 (1970) 2512
34. E. Ortiz-Islas, T. López, R. Gomez and J. Navarrete, *J. Sol-Gel Sci. Technol.* 37 (2006) 165
35. A.C.F.M. Costa, M.A. Vilar, H.L. Lira, R.H.G.A. Kiminami and L. Gama, *Cerâmica* 52 (2006) 255
36. R. Thakkar and U. Chudasama, *Electrochim. Acta* 54 (2009) 2720
37. S.B. Moon, A. Xidis and V.D. Neff, *J. Phys. Chem.* 97 (1993) 1634
38. K.R. Karlin, *Prog. in Inorg. Chem.* 45 (1997) 288
39. E.P. Barrett, L. Joyner and P.P. Halenda, *J. Am. Chem. Soc.* 73 (1951) 373
40. W.M. Azevedo, I.L. Matos and M. Navarro, *J. Mater. Sci. - Mater. Electron.* 17 (2006) 367
41. D.R. Do Carmo, R.M. Silva and N.R. Stradiotto, *Ecletica Quim.* 27 (2002) 197
42. D. Jayasri and S.S. Narayanan, *Sens. Actuators B* 119 (2006) 135
43. A.J. Bard and L.R. Faulkner, *Electrochem. Methods*, Wiley, (1980) 95
44. T.R. Ralph, M.L. Hitchman, J.P. Millington and F.C. Walsh, *J. Electroanal. Chem.* 375 (1994) 1
45. W. Hou and E. Wang, *J. Electroanal. Chem.* 316 (1991) 155